

Λ_s CDM model: A promising scenario for alleviation of cosmological tensions

Özgür Akarsu,^{1,*} Eleonora Di Valentino,^{2,†} Suresh Kumar,^{3,‡}
Rafael C. Nunes,^{4,5,§} J. Alberto Vazquez,^{6,¶} and Anita Yadav^{3,**}

¹*Department of Physics, Istanbul Technical University, Maslak 34469 Istanbul, Turkey*

²*School of Mathematics and Statistics, University of Sheffield,
Hounsfield Road, Sheffield S3 7RH, United Kingdom*

³*Department of Mathematics, Indira Gandhi University, Meerpur, Haryana 122502, India*

⁴*Instituto de Física, Universidade Federal do Rio Grande do Sul, 91501-970 Porto Alegre RS, Brazil*

⁵*Divisão de Astrofísica, Instituto Nacional de Pesquisas Espaciais,*

Avenida dos Astronautas 1758, São José dos Campos, 12227-010, SP, Brazil

⁶*Instituto de Ciencias Físicas, Universidad Nacional Autónoma de México, Cuernavaca, Morelos, 62210, México*

We present a comprehensive analysis of the Λ_s CDM model, which explores the recent conjecture suggesting a rapid transition of the Universe from anti-de Sitter vacua to de Sitter vacua (viz., the cosmological constant switches sign from negative to positive) at redshift $z_{\dagger} \sim 2$, inspired by the graduated dark energy (gDE) model. Our analysis shows that, predicting $z_{\dagger} \approx 1.7$, Λ_s CDM simultaneously addresses the major cosmological tensions of the standard Λ CDM model, viz., the Hubble constant H_0 , the Type Ia Supernovae absolute magnitude M_B , and the growth parameter S_8 tensions, along with other less significant tensions such as the BAO Lyman- α discrepancy.

Introduction – The standard Lambda Cold Dark Matter (Λ CDM) scenario provides a wonderful fit for the majority of astrophysical and cosmological observations carried out over the past decades. However up to recently, in the new era of high-precision cosmology, some discrepancies became statistically significant while analyzing different data sets, placing it in a crossroad. This pivotal situation has compelled the scientific community to embark on a quest for alternative explanations, either rooted in novel physics or by the identification of potential systematic errors in the data. See [1–4] for recent reviews.

The most statistically significant disagreement is in the value of the Hubble constant, H_0 , between the Planck-Cosmic Microwave Background (CMB) [5] estimate, assuming the standard Λ CDM model, and the direct local distance ladder measurements conducted by the SH0ES team [6–8], reaching a significance of more than 5σ . Nevertheless the lower value of H_0 derived from the Planck-CMB data is in agreement with Baryon Acoustic Oscillations (BAO)+Big Bang Nucleosynthesis (BBN) [9, 10], and also with other CMB experiments such as ACT-DR4 and SPT-3G [11, 12]. Conversely, the higher value of H_0 found by SH0ES based on the Supernovae calibrated by Cepheids is in agreement with all the local H_0 measurements [13–19]. Recent reanalysis of the Tip of the Red Giant Branch (TRGB) sample also shows that these local distance indicators are consistent with values of H_0 from Cepheids [20, 21]. Also, it has been argued that the H_0 tension is in fact a tension on the Type Ia Supernovae (SNIa) absolute magnitude M_B [22–24], because the SH0ES H_0 measurement comes directly from M_B estimates.

On the other hand, within the framework of Λ CDM, the CMB measurements from Planck and ACT-DR4 [25] indicate values of $S_8 = \sigma_8 \sqrt{\Omega_m}/0.3$ that exhibit a 1.7σ – 3σ tension with those inferred from various weak lensing [26–

32], galaxy clustering, and redshift-space distortion measurements (see [2, 3, 33–36]). While the status of the S_8 discrepancy may be somewhat less definitive compared to the H_0 tension, there is a clear trend of lower structure growth from low redshift Large Scale Structure probes compared to CMB. Several other tensions and anomalies have recently emerged in the literature, e.g., BAO-Ly- α discrepancies, physical baryon density anomalies, age of the Universe issues, among others [2, 3]. Although individually these tensions may not be very significant, when considered collectively, they could point to the existence of missing components in the current standard cosmological model. The search for a satisfactory explanation for these discrepancies, tensions and anomalies, either through systematic effects in data or new physics, has been a central theme in cosmology over the past few years.

In this *Letter*, we present an observational investigation of the sign-switching Lambda Cold Dark Matter (Λ_s CDM) model, which takes into account the possibility that the Universe has recently, at redshift $z \sim 2$, undergone a phase of rapid transition from anti-de Sitter (AdS) vacua to de Sitter (dS) vacua (viz., the cosmological constant switches sign) [37–39]. We show that this theory-framework can simultaneously resolve the major cosmological tensions, viz., the H_0 , M_B , and S_8 tensions, currently present in Λ CDM. If these tensions grow in significance with new and future data, and in the absence of clear systematic effects explaining their origins, we should look at Λ_s CDM as a candidate that can direct us towards a new standard model of cosmology.

Λ_s CDM model – The Λ_s CDM model is inspired by the recent conjecture that the universe went through a spontaneous AdS-dS transition characterized by a sign-switching cosmological constant (Λ_s) at $z \sim 2$ [37–39]. This conjecture was proposed following the promising observational findings in the graduated dark energy (gDE)

model, which showed that its density smoothly transitioning from negative to positive values rapidly enough at $z \sim 2$ can simultaneously address the H_0 and BAO-Ly- α discrepancies [37]. The theoretical advantages of Λ_s over gDE further bolstered this conjecture [38, 39]. The simplest Λ_s CDM model was constructed phenomenologically by replacing the cosmological constant (Λ) of the standard Λ CDM model with an abrupt sign-switching cosmological constant (Λ_s) at a redshift z_\dagger , which comes as the only additional free parameter. The present-day value of Λ_s is denoted as Λ_{s0} , and the replacement is defined as:

$$\Lambda \rightarrow \Lambda_s \equiv \Lambda_{s0} \operatorname{sgn}[z_\dagger - z], \quad (1)$$

where the sign-switching transition of Λ_s is implemented by the signum function (sgn), which should be taken as an idealized description of a rapid transition phenomenon, such as a phase transition, from AdS vacua provided by $-\Lambda_{s0}$ to dS vacua provided by Λ_{s0} , or DE models such as gDE that can mimic this behavior [39].

The Λ_s CDM model was first analysed using the Planck CMB data, followed by the inclusion of the full BAO data up to $z = 2.36$ (viz., Ly- α DR14, BAO-Galaxy consensus, MGS and 6dFGS) in [38]. It was shown that its consistency with CMB provides H_0 and M_B values that are inversely correlated with z_\dagger . Specifically, the analysis found that for $z_\dagger \sim 1.6$, the model predicts values of $H_0 \approx 73.4 \text{ km s}^{-1} \text{ Mpc}^{-1}$ and $M_B \approx -19.25 \text{ mag}$, in excellent agreement with the SH0ES measurements [6, 40]. Additionally, provided that $z_\dagger \lesssim 2.3$, it achieves an excellent fit to the Ly- α data. This was explained because Λ_s CDM is exactly Λ CDM, except having $\Lambda_s = -\Lambda_{s0} < 0$ for $z > z_\dagger$ (thereby respects the internal consistency of the SH0ES H_0 estimates utilizing M_B and leaves the standard pre-recombination universe untouched), and the fact that the comoving angular diameter distance to last scattering $D_M(z_*) = c \int_0^{z_*} H^{-1} dz$ ($z_* \approx 1090$) is strictly fixed by the CMB power spectra, a reduction in $H(z)$ for $z > z_\dagger$ compared to Λ CDM must be compensated by an enhancement in $H(z)$ for $z < z_\dagger$ resulting in higher H_0 and fainter M_B . It turns out that, being consistent with Planck CMB for $z_\dagger \gtrsim 1.5$, Λ_s CDM simultaneously ameliorates the H_0 , M_B , and S_8 tensions, though the inclusion of full BAO data in the analysis compromises the model's success by moving z_\dagger to ~ 2.4 —in this case the negative cosmological constant, $\Lambda_s(z > z_\dagger) = -\Lambda_{s0}$, does not have enough time to significantly influence the evolution of the universe against the dust still dominating the universe.

This analysis was elaborated by using the Pantheon SNIa data [41] (to break the degeneracy between H_0 and z_\dagger , without using BAO), both with and without the SH0ES M_B prior [23], and/or the *completed* BAO data [42] along with Planck CMB in [39]. It was shown that when the M_B prior is utilized without the full BAO data, predicting $z_\dagger \sim 1.8$, Λ_s CDM reduces all the major discrepancies (related to H_0 , M_B , and S_8) that prevail

within Λ CDM (and its canonical extensions) below $\sim 1\sigma$, and is very strongly favored over Λ CDM in terms of Bayesian evidence. It is worth noting that the presence of sign-switching at $z_\dagger \sim 2$ was originally motivated by BAO Ly- α (which favors negative/zero DE densities for $z \gtrsim 2$) in [37] and then this was further supported in [38] by showing that while the BAO Ly- α insists on $z_\dagger \lesssim 2.3$, the galaxy BAO from $z_{\text{eff}} = 0.38$ is in opposition to this pushing z_\dagger to values larger than 2. Pleasantly, the results in [39] show that the presence of the M_B prior finds excellent constraints of $z_\dagger \sim 2$ ($z_\dagger \sim 1.8$ when full BAO data is not included) even when BAO Ly- α is not used. A close inspection of the fact that using full BAO data hinders the success of Λ_s CDM in [39] shows that Λ_s CDM is discrepant with the galaxy BAO data from $z_{\text{eff}} = 0.15$ and 0.38. Accordingly, to reconcile Λ_s CDM with these two galaxy BAO data as well, adding correction to it might be an option (e.g., by introducing wavelet-type corrections to the Hubble radius of Λ_s CDM at low redshifts, as suggested in [43]), which, however, would come at the cost of introducing additional free parameters. Alternatively, this can be related to the discordance between low- and high-redshift BAO measurements in Λ_s CDM, which is also present in Λ CDM [44, 45].

In this paper, we further investigate the Λ_s CDM model by using updated and extended data. To achieve this, along with Planck CMB data [46], we utilize the recent Pantheon+ SNe Ia sample [47], and additionally the 2D BAO data [48, 49], as a less model dependent alternative to 3D BAO data used in previous analyses of Λ_s CDM. Furthermore, for a robust assessment of the resolution of the S_8 tension within Λ_s CDM, we use cosmic shear measurements obtained from the latest public data release of the Kilo-Degree Survey (KiDS-1000) [29]. This inclusion allows us to robustly determine its consistency with regards to amplitude and growth of structures. By combining these diverse data sets, we aim to provide a comprehensive analysis that further establishes the viability and robustness of Λ_s CDM in addressing various cosmological tensions and discrepancies.

Data sets and Methodology – We describe below the observational data sets and the statistical methods used to explore the parameter space. *CMB*: The full Planck 2018 temperature and polarization likelihood [46] in combination with the Planck 2018 lensing likelihood [50]. We refer to this data set as Planck. *Transversal BAO*: Measurements of 2D BAO, $\theta_{\text{BAO}}(z)$, obtained in a weakly model-dependent approach, compiled in Table I in [48, 49]. These measurements were obtained using public data releases (DR) of the Sloan Digital Sky Survey (SDSS), namely: DR7, DR10, DR11, DR12, DR12Q (quasars), and following the same methodology in all measurements. The main differences (methodology and sample) between the 3D and 2D BAO measurements are discussed in [51, 52] and references therein. We refer to this data set as BAOtr. *Type Ia supernovae and Cepheids*: We use the SNe Ia

distance moduli measurements from the Pantheon+ sample [47], which consists of 1701 light curves of 1550 distinct SNe Ia ranging in the redshift interval $z \in [0.001, 2.26]$. We refer to this dataset as PantheonPlus. We also consider the SH0ES Cepheid host distance anchors, which facilitate constraints on both M_B and H_0 . When utilizing SH0ES Cepheid host distances, the SNe Ia distance residuals are modified following the relationship Eq.(14) of [47]. We refer to this dataset as PantheonPlus&SH0ES. *Cosmic Shear*: We use KiDS-1000 data [53, 54]. This includes the weak lensing two-point statistics data for both the auto and cross-correlations across five tomographic redshift bins [55]. We employ the public likelihood in [56]. We follow the KiDS team analysis and adopt the COSEBIs (Complete Orthogonal Sets of E/B-Integrals) likelihood in our results [29]. For the prediction of the matter power spectrum, we use the augmented halo model code, HMcode [57]. We highlight that at level of the linear perturbations theory and Boltzmann equations, Λ_s CDM have exactly the same shape as predicted by Λ CDM. The only effect on the matter power spectrum comes from the $H(z)$ behavior at late times. As HMcode is robustly tested at percent level for variation on $H(z)$ functions beyond Λ CDM, we conclude that no further change on the HMcode is necessary to apply cosmic shear measurements on Λ_s CDM. We refer to this data set as KiDS-1000.

We explore the full parameter space of the Λ_s CDM model and, for comparison, that of Λ CDM. The baseline seven free parameters of Λ_s CDM are given by $\mathcal{P} = \{\omega_b, \omega_c, \theta_s, A_s, n_s, \tau_{\text{reio}}, z_{\dagger}\}$, where the first six are the common ones with Λ CDM. We use CLASS+MontePython code [58–60] with Metropolis-Hastings mode to derive constraints on cosmological parameters for Λ_s CDM baseline from several combinations of the data sets defined above, ensuring a Gelman-Rubin convergence criterion [61] of $R - 1 < 10^{-2}$ in all the runs. For the model comparison, we compute the relative log-Bayesian evidence $\ln \mathcal{B}_{ij}$ to estimate the Evidence of Λ_s CDM with respect to Λ CDM, through the publicly available package MCEvidence [62] [63, 64]. We use the convention of a negative value if Λ_s CDM is preferred against Λ CDM, or vice versa, and we refer to the revised Jeffreys’ scale by Trotta [65, 66], to interpret the results. We will say that the evidence is inconclusive if $0 \leq |\ln \mathcal{B}_{ij}| < 1$, weak if $1 \leq |\ln \mathcal{B}_{ij}| < 2.5$, moderate if $2.5 \leq |\ln \mathcal{B}_{ij}| < 5$, strong if $5 \leq |\ln \mathcal{B}_{ij}| < 10$, and very strong if $|\ln \mathcal{B}_{ij}| \geq 10$.

Results – We present, in Table I, the 68% CL constraints on the main cosmological parameters of interest of the Λ_s CDM and Λ CDM models obtained in our analyses by using different combinations of data sets, while we provide the complete table for the entire parameter space of the two models in the *Supplemental Material*. When we consider only Planck data, we notice that the characteristic parameter of the Λ_s CDM model, z_{\dagger} , remains unconstrained, and we find strong degeneracy with other derived parameters, especially with H_0 and Ω_m ,

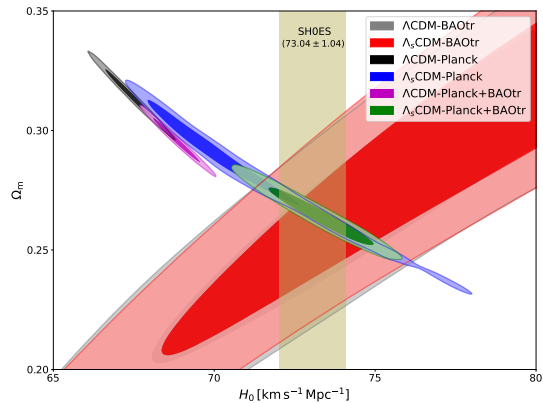


FIG. 1. 2D contours at 68% and 95% CLs in the H_0 - Ω_m plane for the Λ_s CDM and Λ CDM models from the Planck and/or BAOtr data. It deserves mention that, in case of Λ_s CDM, the Planck and BAOtr contours intersect right on the vertical band of SH0ES measurement.

increasing values in H_0 and decreasing the total matter density parameter today. To break the degeneracy, we include the BAOtr data in our analysis with Planck data, which enables the constraint: $z_{\dagger} = 1.70^{+0.09}_{-0.19}$. Interestingly, this inclusion of BAOtr data leads to a higher value of the Hubble constant, viz., $H_0 = 73.3^{+1.2}_{-1.0} \text{ km s}^{-1} \text{ Mpc}^{-1}$ which is perfectly consistent with the SH0ES measurement $H_0 = 73.04 \pm 1.04 \text{ km s}^{-1} \text{ Mpc}^{-1}$ [6]. In particular, it is noteworthy to observe in Fig. 1 that the two models yield almost the identical contours for the BAOtr data (along with BBN prior $10^2 \omega_b^{\text{LUNA}} = 2.233 \pm 0.036$ [67]), while the BAOtr and Planck contours disagree in the case of Λ CDM; however, when considering Λ_s CDM, it is striking that the BAOtr and Planck contours precisely intersect at the vertical band of SH0ES H_0 measurement. Considering this remarkable success of Λ_s CDM in addressing the H_0 tension, we proceed to incorporate the new PantheonPlus (PP) sample into our analysis, both with and without the Cepheids calibration provided by SH0ES. From the combination of the Planck, BAOtr, and PantheonPlus data sets, we find the constraints: $z_{\dagger} = 1.87^{+0.13}_{-0.21}$ and $H_0 = 71.72^{+0.73}_{-0.92} \text{ km s}^{-1} \text{ Mpc}^{-1}$. This constraint on H_0 is again consistent with the SH0ES measurement. Based on this finding, we confidently include the calibration provided by SH0ES, leaving our conclusions unchanged. We also note that the discrepancy in M_B between the SH0ES data ($M_B = -19.244 \pm 0.037 \text{ mag}$) and the base Λ CDM cosmology inferred from Planck ($M_B = -19.401 \pm 0.027 \text{ mag}$) is here resolved within the framework of Λ_s CDM model. Thus, the Λ_s CDM model also provides a robust solution to the M_B tension.

From the results of these analyses, we further notice that S_8 and Ω_m get lower values in Λ_s CDM compared to Λ CDM. In order to see whether S_8 tension is resolved in our model, we separately analyse the models with KiDS-

TABLE I. Marginalized constraints, mean values with 68% CL (bestfit value), on the free and some derived parameters of the Λ_s CDM and standard Λ CDM models for different data set combinations. Bayes factors \mathcal{B}_{ij} given by $\ln \mathcal{B}_{ij} = \ln \mathcal{Z}_{\Lambda\text{CDM}} - \ln \mathcal{Z}_{\Lambda_s\text{CDM}}$ are also displayed for the different analyses so that a negative value indicates a preference for the Λ_s CDM model against the Λ CDM scenario.

Data set	Planck	Planck+BAOtr	Planck+BAOtr+PP	Planck+BAOtr+PP&SH0ES	Planck+BAOtr+PP&SH0ES+KiDS-1000
Model	Λ_s CDM Λ CDM	Λ_s CDM Λ CDM	Λ_s CDM Λ CDM	Λ_s CDM Λ CDM	Λ_s CDM Λ CDM
z_{\dagger}	unconstrained	$1.70^{+0.09}_{-0.19}$ (1.65)	$1.87^{+0.13}_{-0.21}$ (1.75)	$1.70^{+0.10}_{-0.13}$ (1.67)	$1.72^{+0.09}_{-0.12}$ (1.70)
M_B [mag]	--	--	$-19.317^{+0.021}_{-0.025}$ (-19.311)	-19.290 ± 0.017 (-19.278)	-19.282 ± 0.017 (-19.280)
	--	--	-19.407 ± 0.013 (-19.411)	-19.379 ± 0.012 (-19.373)	-19.372 ± 0.011 (-19.369)
H_0 [km/s/Mpc]	$70.77^{+0.79}_{-2.70}$ (71.22) 67.39 ± 0.55 (67.28)	$73.30^{+1.20}_{-1.00}$ (73.59) 68.84 ± 0.48 (68.61)	$71.72^{+0.73}_{-0.93}$ (71.97) 68.55 ± 0.44 (68.54)	72.82 ± 0.65 (73.20) 69.57 ± 0.42 (69.73)	73.16 ± 0.64 (73.36) 69.83 ± 0.37 (69.96)
Ω_m	$0.2860^{+0.0230}_{-0.0099}$ (0.2796) 0.3151 ± 0.0075 (0.3163)	$0.2643^{+0.0072}_{-0.0063}$ (0.2618) 0.2958 ± 0.0061 (0.2984)	$0.2768^{+0.0072}_{-0.0063}$ (0.2759) 0.2995 ± 0.0056 (0.2992)	0.2683 ± 0.0052 (0.2646) 0.2869 ± 0.0051 (0.2849)	0.2646 ± 0.0052 (0.2622) 0.2837 ± 0.0045 (0.2816)
S_8	$0.801^{+0.026}_{-0.016}$ (0.791) 0.832 ± 0.013 (0.835)	0.777 ± 0.011 (0.772) 0.802 ± 0.011 (0.804)	0.791 ± 0.011 (0.794) 0.808 ± 0.010 (0.804)	0.783 ± 0.010 (0.777) 0.788 ± 0.010 (0.784)	0.774 ± 0.009 (0.773) 0.781 ± 0.008 (0.782)
χ^2_{\min}	2778.06 2780.52	2793.38 2820.30	4219.68 4235.18	4097.32 4138.26	4185.34 4226.50
$\ln \mathcal{B}_{ij}$	-1.28	-12.65	-7.52	-19.47	-19.77

1000 only data. The upper panels of Fig. 2 show 2D contours at 68%, and 95% CLs in the Ω_m - S_8 plane for the Λ_s CDM and Λ CDM models. We note that the two models yield very similar contours for the KiDS data (as both models being the same at redshifts relevant to KiDS data). However, while the Planck and KiDS contours disagree in Λ CDM, they do agree in Λ_s CDM as the Planck contour extends directly into the KiDS contour. This occurs because the smaller z_{\dagger} values allowed by Planck data lead to smaller values of S_8 and Ω_m . For Λ_s CDM, the

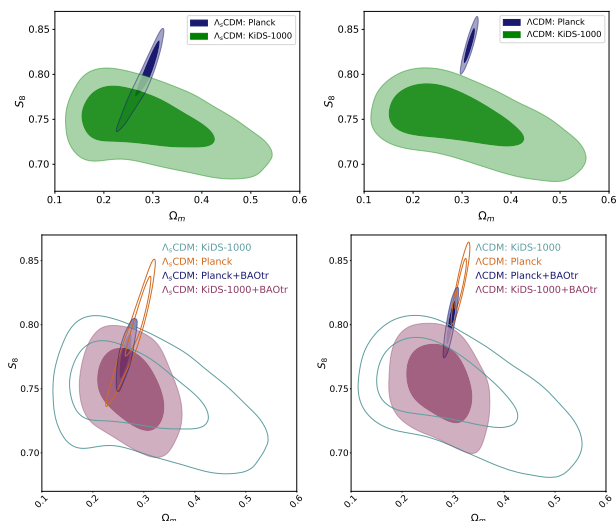


FIG. 2. 2D contours at 68% and 95% CLs in the Ω_m - S_8 plane for the Λ_s CDM and Λ CDM models. $S_8 = 0.801^{+0.026}_{-0.016}$ (Λ_s CDM: Planck), $S_8 = 0.746^{+0.026}_{-0.021}$ (Λ_s CDM: KiDS-1000), $S_8 = 0.832 \pm 0.013$ (Λ CDM: Planck), $S_8 = 0.749^{+0.027}_{-0.020}$ (Λ CDM: KiDS-1000) at 68% CL.

observational constraints on S_8 , viz., $S_8 = 0.801^{+0.026}_{-0.016}$ from Planck and $S_8 = 0.746^{+0.026}_{-0.021}$ from KiDS-1000, are compatible with each other, and thus the S_8 tension does not exist in Λ_s CDM while it prevails in Λ CDM. The contour plots for Λ_s CDM in the lower left panel of Fig. 2 (see the lower right panel for Λ CDM) further show the robustness of the constraints on S_8 in the presence of other data sets under consideration.

Finally, from the analysis of the models using the combination of all the data sets under consideration, viz., Planck+BAOtr+PP&SH0ES+KiDS-1000, we obtain the most robust constraints on the model parameters as shown in the last column of Table I. Fig. 3 shows the whisker plot displaying 68% CL constraints on H_0 for the Λ_s CDM and Λ CDM models from various data combinations. We see that there is no H_0 tension in the present analyses of Λ_s CDM with all data combinations including the BAOtr data. We emphasize that all data sets under consideration are compatible within the framework of Λ_s CDM. Note that there is no H_0 tension in our results using the BAOtr data, while using 3D BAO data Λ_s CDM reduces the H_0 tension but fails to fully resolve it in previous works [38, 39]. We attribute this to the possible model dependence of the 3D BAO reconstruction, which is (mostly) absent for the BAOtr data. In particular, [39] finds that the two galaxy 3D BAO data—viz., SDSS main galaxy sample (MGS) from $z_{\text{eff}} = 0.15$ and BOSS galaxy from $z_{\text{eff}} = 0.38$ —are responsible for this reduced concordance under Λ_s CDM.

In addition, as can be seen in *Supplemental Material*, Λ_s CDM poses no problems with any of the well-known parameters of the Universe based on observations and, on theoretical side, standard physics. Instead, the constraints on its six baseline parameters that are common with Λ CDM, show unprecedented stability in the face

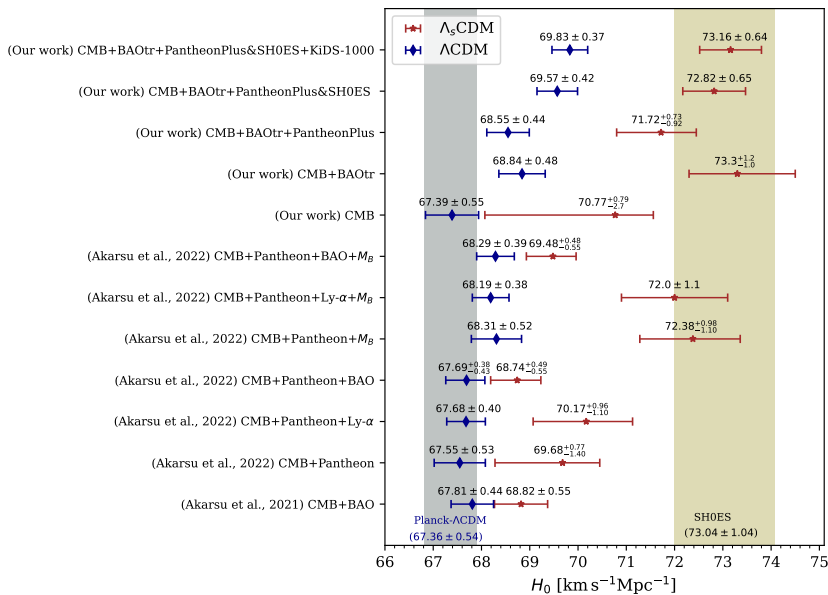


FIG. 3. The mean values with 68% CL on H_0 for the Λ_s CDM and Λ CDM models from various data combinations. The left vertical band stands for Planck- Λ CDM constraint: $H_0 = 67.36 \pm 0.54 \text{ km s}^{-1} \text{ Mpc}^{-1}$, and the right one is for the latest SH0ES measurement [6]: $H_0 = 73.04 \pm 1.04 \text{ km s}^{-1} \text{ Mpc}^{-1}$. We see that there is no H_0 tension in most data combinations for Λ_s CDM, in particular, when we use the less model-dependent BAOtr data. The only exception is in the cases explored in previous works [38, 39] that employ the 3D BAO data (BAO in the plot), among which the two galaxy BAO data from $z_{\text{eff}} = 0.15$ and 0.38 preventing the model from successfully resolving the tension.

of different data sets. Moreover, Λ_s CDM is consistent with BAO Ly- α data. It predicts the age of the universe, $t_0 = 13.522 \pm 0.027 \text{ Gyr}$, which is consistent with estimations utilizing the oldest globular clusters, e.g., $t_{\text{u}} = 13.50 \pm 0.15(\text{stat.}) \text{ Gyr}$ [68]. Furthermore, it maintains the physics and dynamics of the pre-recombination universe as they are in the standard model. For example, the constraints on the drag redshift and the sound horizon at this epoch (r_{d} and z_{d}) remain unaltered compared to those obtained within Λ CDM. Additionally, the constraints on Y_{P} (the primordial mass fraction of ^4He) and ω_{b} (the present-day physical density parameter of baryons) are consistent with the standard BBN.

To provide a conclusive assessment of the robustness of our results, we conduct a Bayesian model comparison to evaluate the relative performance of Λ_s CDM and Λ CDM in terms of their statistical fit to the data. The results of the relative Bayesian evidence are presented in the lower section of Table I. According to the revised Jeffreys' scale, the evidence in favor of the Λ_s CDM scenario is found *weak* when considering the Planck data alone. However, it strengthens to a *strong* level in the analysis with Planck+BAOtr+PP data. Remarkably, for all the other combinations of data-sets considered here, the evidence in favor of the Λ_s CDM scenario turns out to be *very strong*. Thus, Λ_s CDM finds by far better statistical fit to the data compared to Λ CDM.

The findings in this study indicate that the Λ_s CDM model consistently outperforms the standard Λ CDM model not only in resolving the prominent cosmological tensions, but also in terms of the statistical fit to the data across various data-set combinations, providing very strong support for its validity and effectiveness in explaining the observed cosmological phenomena. In addition, Λ_s CDM mitigates several other tensions of lower statistical significance, as illustrated in *Supplemental Material*, where we also provide additional information about the main results discussed here.

Final remarks – Using the state-of-the-art methodology for the observational constraints and recent data available in the literature, we show that a simple model, viz., Λ_s CDM [37–39], which experiences a rapid transition of the Universe from anti-de Sitter vacua to de Sitter vacua (namely, the cosmological constant switches sign from negative to positive) at late times ($z_{\text{†}} \approx 1.7$), can address the major cosmological tensions (H_0 , M_{B} , and S_8 tensions) simultaneously; in particular, when we use BAOtr data, which are less model-dependent, unlike the previous works on Λ_s CDM that used 3D BAO data. Our proposal consists of the most economical cosmological model available in the literature with that ability, because it does not involve any extra physical parameters beyond Λ CDM, but only a cosmic time transition which needs to be fixed by data. The abrupt/rapid nature of the Λ_s , or a dark

energy mimicking it, and also the fact that it shifts from negative to positive value, may render finding a concrete physical mechanism underlying this model challenging. However, the phenomenological success of Λ_s CDM despite its simplicity, is highly encouraging to look for possible underlying physical mechanisms; see [37–39] for further discussions and [69] realizing abrupt sign-switching cosmological constant via a classical metric signature change across boundaries with a degenerate metric in different formulations of general relativity. On the other hand, our findings may have far-reaching implications in theoretical physics as negative cosmological constant is a theoretical sweet spot–viz., AdS space/vacuum is welcome due to the AdS/CFT correspondence [70] and is preferred by string theory and string theory motivated supergravities [71]. And thereby, it would be natural to associate this phenomenon to a possible (phase) transition from AdS to dS that is derived in such fundamental theories of physics, and the theories that find motivation from them. Thus, it is essential to conduct further research on refinement at both theoretical and observational level, particularly on identifying observables unique to this model and searching for their traces in the sky, for establishing the Λ_s CDM model as a promising candidate or guide for a new concordance cosmological model of the Universe.

Acknowledgements – This work is dedicated to the memory of Professor John David Barrow. We gratefully acknowledge Marika Asgari for the valuable discussions, inputs in the paper, and help with the KiDS data analysis. We thank Joseph Silk for useful discussions. Ö.A. acknowledges the support by the Turkish Academy of Sciences in scheme of the Outstanding Young Scientist Award (TÜBA-GEBİP). Ö.A. is supported in part by TUBITAK grant 122F124. E.D.V. is supported by a Royal Society Dorothy Hodgkin Research Fellowship. S.K. gratefully acknowledges support from the Science and Engineering Research Board (SERB), Govt. of India (File No. CRG/2021/004658). R.C.N. thanks the CNPq for partial financial support under the project No. 304306/2022-3. J.A.V. acknowledges the support provided by FOSEC SEP-CONACYT Investigación Básica A1-S-21925, Ciencias de Frontera CONACYT-PRONACES/304001/202 and UNAM-DGAPA-PAPIIT IN117723. A.Y. is supported by Junior Research Fellowship (CSIR/UGC Ref. No. 201610145543) from University Grants Commission, Govt. of India. This article is based upon work from COST Action CA21136 Addressing observational tensions in cosmology with systematics and fundamental physics (CosmoVerse) supported by COST (European Cooperation in Science and Technology).

* akarsuo@itu.edu.tr

† e.divalentino@sheffield.ac.uk

- ‡ suresh.math@igu.ac.in
 § rafadcnunes@gmail.com
 ¶ javazquez@icf.unam.mx
 ** anita.math.rs@igu.ac.in
- [1] E. Di Valentino, O. Mena, S. Pan, L. Visinelli, W. Yang, A. Melchiorri, D. F. Mota, A. G. Riess, and J. Silk, *Class. Quant. Grav.* **38**, 153001 (2021), arXiv:2103.01183 [astro-ph.CO].
 - [2] E. Abdalla *et al.*, *JHEAp* **34**, 49 (2022), arXiv:2203.06142 [astro-ph.CO].
 - [3] L. Perivolaropoulos and F. Skara, *New Astron. Rev.* **95**, 101659 (2022), arXiv:2105.05208 [astro-ph.CO].
 - [4] E. Di Valentino, *Universe* **8**, 399 (2022).
 - [5] N. Aghanim *et al.* (Planck), *Astron.Astrophys.* **641**, A6 (2020), arXiv:1807.06209 [astro-ph.CO].
 - [6] A. G. Riess *et al.*, *Astrophys. J. Lett.* **934**, L7 (2022), arXiv:2112.04510 [astro-ph.CO].
 - [7] A. G. Riess, L. Breuval, W. Yuan, S. Casertano, L. M. Macri, J. B. Bowers, D. Scolnic, T. Cantat-Gaudin, R. I. Anderson, and M. C. Reyes, *Astrophys. J.* **938**, 36 (2022), arXiv:2208.01045 [astro-ph.CO].
 - [8] Y. S. Murakami, A. G. Riess, B. E. Stahl, W. D. Kenworthy, D.-M. A. Pluck, A. Macoretta, D. Brout, D. O. Jones, D. M. Scolnic, and A. V. Filippenko, (2023), arXiv:2306.00070 [astro-ph.CO].
 - [9] N. Schöneberg, L. Verde, H. Gil-Marín, and S. Brieden, *JCAP* **11**, 039 (2022), arXiv:2209.14330 [astro-ph.CO].
 - [10] A. Cuceu, J. Farr, P. Lemos, and A. Font-Ribera, *JCAP* **10**, 044 (2019), arXiv:1906.11628 [astro-ph.CO].
 - [11] S. Aiola *et al.* (ACT), *JCAP* **12**, 047 (2020), arXiv:2007.07288 [astro-ph.CO].
 - [12] L. Balkenhol *et al.* (SPT-3G), arXiv:2212.05642 (2022), arXiv:2212.05642 [astro-ph.CO].
 - [13] S. M. Ward *et al.*, arXiv:2209.10558 (2022), arXiv:2209.10558 [astro-ph.CO].
 - [14] K. N. Abazajian *et al.* (CMB-S4), arXiv:1610.02743 (2016), arXiv:1610.02743 [astro-ph.CO].
 - [15] J. L. Sanders, arXiv:2304.01671 (2023), arXiv:2304.01671 [astro-ph.GA].
 - [16] W. L. Freedman, *Astrophys. J.* **919**, 16 (2021), arXiv:2106.15656 [astro-ph.CO].
 - [17] G. S. Anand, R. B. Tully, L. Rizzi, A. G. Riess, and W. Yuan, *Astrophys. J.* **932**, 15 (2022), arXiv:2108.00007 [astro-ph.CO].
 - [18] J. P. Blakeslee, J. B. Jensen, C.-P. Ma, P. A. Milne, and J. E. Greene, *Astrophys. J.* **911**, 65 (2021), arXiv:2101.02221 [astro-ph.CO].
 - [19] T. de Jaeger, L. Galbany, A. G. Riess, B. E. Stahl, B. J. Shappee, A. V. Filippenko, and W. Zheng, *Mon. Not. Roy. Astron. Soc.* **514**, 4620 (2022), arXiv:2203.08974 [astro-ph.CO].
 - [20] R. I. Anderson, N. W. Koblishcke, and L. Eyer, arXiv:2303.04790 (2023), arXiv:2303.04790 [astro-ph.CO].
 - [21] D. Scolnic, A. G. Riess, J. Wu, S. Li, G. S. Anand, R. Beaton, S. Casertano, R. Anderson, S. Dhawan, and X. Ke, arXiv:2304.06693 (2023), arXiv:2304.06693 [astro-ph.CO].
 - [22] G. Efstathiou, *Mon. Not. Roy. Astron. Soc.* **505**, 3866 (2021), arXiv:2103.08723 [astro-ph.CO].
 - [23] D. Camarena and V. Marra, *Mon. Not. Roy. Astron. Soc.* **504**, 5164 (2021), arXiv:2101.08641 [astro-ph.CO].
 - [24] R. C. Nunes and E. Di Valentino, *Phys. Rev. D* **104**, 063529 (2021), arXiv:2107.09151 [astro-ph.CO].

- [25] S. Aiola *et al.* (ACT), *JCAP* **12**, 047 (2020), [arXiv:2007.07288 \[astro-ph.CO\]](#).
- [26] L. F. Secco *et al.* (DES), *Phys. Rev. D* **105**, 023515 (2022), [arXiv:2105.13544 \[astro-ph.CO\]](#).
- [27] A. Amon *et al.* (DES), *Phys. Rev. D* **105**, 023514 (2022), [arXiv:2105.13543 \[astro-ph.CO\]](#).
- [28] T. M. C. Abbott *et al.* (DES), [arXiv:2207.05766 \(2022\)](#), [arXiv:2207.05766 \[astro-ph.CO\]](#).
- [29] M. Asgari *et al.* (KiDS), *Astron. Astrophys.* **645**, A104 (2021), [arXiv:2007.15633 \[astro-ph.CO\]](#).
- [30] X. Li *et al.*, [arXiv:2304.00702 \(2023\)](#), [arXiv:2304.00702 \[astro-ph.CO\]](#).
- [31] R. Dalal *et al.*, [arXiv:2304.00701 \(2023\)](#), [arXiv:2304.00701 \[astro-ph.CO\]](#).
- [32] T. M. C. Abbott *et al.* (Kilo-Degree Survey, Dark Energy Survey), (2023), [arXiv:2305.17173 \[astro-ph.CO\]](#).
- [33] E. Di Valentino *et al.*, *Astropart. Phys.* **131**, 102604 (2021), [arXiv:2008.11285 \[astro-ph.CO\]](#).
- [34] R. C. Nunes and S. Vagnozzi, *Monthly Notices of the Royal Astronomical Society* **505**, 5427–5437 (2021).
- [35] C. Heymans *et al.*, *Astron. Astrophys.* **646**, A140 (2021), [arXiv:2007.15632 \[astro-ph.CO\]](#).
- [36] S. Sugiyama, H. Miyatake, S. More, X. Li, M. Shirasaki, M. Takada, Y. Kobayashi, R. Takahashi, T. Nishimichi, A. J. Nishizawa, M. M. Rau, T. Zhang, R. Dalal, R. Mandelbaum, M. A. Strauss, T. Hamana, M. Oguri, K. Osato, A. Kannawadi, R. Armstrong, Y. Komiyama, R. H. Lupton, N. B. Lust, S. Miyazaki, H. Murayama, Y. Okura, P. A. Price, P. J. Tait, M. Tanaka, and S.-Y. Wang, [arXiv e-prints](#), [arXiv:2304.00705 \(2023\)](#), [arXiv:2304.00705 \[astro-ph.CO\]](#).
- [37] O. Akarsu, J. D. Barrow, L. A. Escamilla, and J. A. Vazquez, *Phys. Rev. D* **101**, 063528 (2020), [arXiv:1912.08751 \[astro-ph.CO\]](#).
- [38] O. Akarsu, S. Kumar, E. Özüiker, and J. A. Vazquez, *Phys. Rev. D* **104**, 123512 (2021), [arXiv:2108.09239 \[astro-ph.CO\]](#).
- [39] O. Akarsu, S. Kumar, E. Özüiker, J. A. Vazquez, and A. Yadav, *Phys. Rev. D* **108**, 023513 (2023), [arXiv:2211.05742 \[astro-ph.CO\]](#).
- [40] D. Camarena and V. Marra, *Mon. Not. Roy. Astron. Soc.* **504**, 5164 (2021), [arXiv:2101.08641 \[astro-ph.CO\]](#).
- [41] D. M. Scolnic *et al.* (Pan-STARRS1), *Astrophys. J.* **859**, 101 (2018), [arXiv:1710.00845 \[astro-ph.CO\]](#).
- [42] S. Alam *et al.* (eBOSS), *Phys. Rev. D* **103**, 083533 (2021), [arXiv:2007.08991 \[astro-ph.CO\]](#).
- [43] O. Akarsu, E. O. Colgain, E. Özüiker, S. Thakur, and L. Yin, *Phys. Rev. D* **107**, 123526 (2023), [arXiv:2207.10609 \[astro-ph.CO\]](#).
- [44] E. Aubourg *et al.*, *Phys. Rev. D* **92**, 123516 (2015), [arXiv:1411.1074 \[astro-ph.CO\]](#).
- [45] H. du Mas des Bourboux *et al.*, *Astrophys. J.* **901**, 153 (2020), [arXiv:2007.08995 \[astro-ph.CO\]](#).
- [46] N. Aghanim *et al.* (Planck), *Astron. Astrophys.* **641**, A5 (2020), [arXiv:1907.12875 \[astro-ph.CO\]](#).
- [47] D. Brout *et al.*, *Astrophys. J.* **938**, 110 (2022), [arXiv:2202.04077 \[astro-ph.CO\]](#).
- [48] R. C. Nunes, S. K. Yadav, J. F. Jesus, and A. Bernui, *Mon. Not. Roy. Astron. Soc.* **497**, 2133 (2020), [arXiv:2002.09293 \[astro-ph.CO\]](#).
- [49] E. de Carvalho, A. Bernui, F. Avila, C. P. Novaes, and J. P. Nogueira-Cavalcante, *Astron. Astrophys.* **649**, A20 (2021), [arXiv:2103.14121 \[astro-ph.CO\]](#).
- [50] N. Aghanim *et al.* (Planck), *Astron. Astrophys.* **641**, A8 (2020), [arXiv:1807.06210 \[astro-ph.CO\]](#).
- [51] A. Bernui, E. D. Valentino, W. Giarè, S. Kumar, and R. C. Nunes, *Physical Review D* **107** (2023), [10.1103/physrevd.107.103531](#).
- [52] R. C. Nunes and A. Bernui, *The European Physical Journal C* **80** (2020), [10.1140/epjc/s10052-020-08601-8](#).
- [53] K. Kuijken *et al.*, *Astron. Astrophys.* **625**, A2 (2019), [arXiv:1902.11265 \[astro-ph.GA\]](#).
- [54] B. Giblin *et al.*, *Astron. Astrophys.* **645**, A105 (2021), [arXiv:2007.01845 \[astro-ph.CO\]](#).
- [55] H. Hildebrandt *et al.*, *Astron. Astrophys.* **647**, A124 (2021), [arXiv:2007.15635 \[astro-ph.CO\]](#).
- [56] KiDS-1000 Montepython likelihood.
- [57] A. Mead, J. Peacock, C. Heymans, S. Joudaki, and A. Heavens, *Mon. Not. Roy. Astron. Soc.* **454**, 1958 (2015), [arXiv:1505.07833 \[astro-ph.CO\]](#).
- [58] D. Blas, J. Lesgourgues, and T. Tram, *JCAP* **07**, 034 (2011), [arXiv:1104.2933 \[astro-ph.CO\]](#).
- [59] J. Lesgourgues, [arXiv:1104.2932 \(2011\)](#), [arXiv:1104.2932 \[astro-ph.IM\]](#).
- [60] T. Brinckmann and J. Lesgourgues, *Phys. Dark Univ.* **24**, 100260 (2019), [arXiv:1804.07261 \[astro-ph.CO\]](#).
- [61] A. Gelman and D. B. Rubin, *Statist. Sci.* **7**, 457 (1992).
- [62] [github.com/yabebalFantaye/MCEvidence](#).
- [63] A. Heavens, Y. Fantaye, E. Sellentin, H. Eggers, Z. Hosenie, S. Kroon, and A. Mootoovaloo, *Phys. Rev. Lett.* **119**, 101301 (2017), [arXiv:1704.03467 \[astro-ph.CO\]](#).
- [64] A. Heavens, Y. Fantaye, A. Mootoovaloo, H. Eggers, Z. Hosenie, S. Kroon, and E. Sellentin, [arXiv:1704.03472 \(2017\)](#), [arXiv:1704.03472 \[stat.CO\]](#).
- [65] R. E. Kass and A. E. Raftery, *J. Am. Statist. Assoc.* **90**, 773 (1995).
- [66] R. Trotta, *Contemp. Phys.* **49**, 71 (2008), [arXiv:0803.4089 \[astro-ph\]](#).
- [67] V. Mossa *et al.*, *Nature* **587**, 210 (2020).
- [68] D. Valcin, R. Jimenez, L. Verde, J. L. Bernal, and B. D. Wandelt, *JCAP* **08**, 017 (2021), [arXiv:2102.04486 \[astro-ph.GA\]](#).
- [69] B. Alexandre, S. Gielen, and J. a. Magueijo, (2023), [arXiv:2306.11502 \[hep-th\]](#).
- [70] J. M. Maldacena, *Adv. Theor. Math. Phys.* **2**, 231 (1998), [arXiv:hep-th/9711200](#).
- [71] R. Bouso and J. Polchinski, *JHEP* **06**, 006 (2000), [arXiv:hep-th/0004134](#).

Supplemental material

Özgür Akarsu,^{1,*} Eleonora Di Valentino,^{2,†} Suresh Kumar,^{3,‡}
Rafael C. Nunes,^{4,5,§} J. Alberto Vazquez,^{6,¶} and Anita Yadav^{3,**}

¹*Department of Physics, Istanbul Technical University, Maslak 34469 Istanbul, Turkey*

²*School of Mathematics and Statistics, University of Sheffield,
Hounsfield Road, Sheffield S3 7RH, United Kingdom*

³*Department of Mathematics, Indira Gandhi University, Meerpur, Haryana 122502, India*

⁴*Instituto de Física, Universidade Federal do Rio Grande do Sul, 91501-970 Porto Alegre RS, Brazil*

⁵*Divisão de Astrofísica, Instituto Nacional de Pesquisas Espaciais,*

Avenida dos Astronautas 1758, São José dos Campos, 12227-010, SP, Brazil

⁶*Instituto de Ciencias Físicas, Universidad Nacional Autónoma de México, Cuernavaca, Morelos, 62210, México*

MODEL BASELINE AND PRIOR INFO

The baseline seven free parameters of Λ_s CDM are given by $\mathcal{P} = \{\omega_b, \omega_c, \theta_s, A_s, n_s, \tau_{\text{reio}}, z_{\dagger}\}$, where the first six are the common ones with Λ CDM, viz., $\omega_b = \Omega_b h^2$ and $\omega_c = \Omega_c h^2$ (Ω being the present-day density parameter) are, respectively, the present-day physical density parameters of baryons and CDM, θ_s is the ratio of the sound horizon to the angular diameter distance at decoupling, A_s is the initial super-horizon amplitude of curvature perturbations at $k = 0.05 \text{ Mpc}^{-1}$, n_s is the primordial spectral index, and τ_{reio} is the reionization optical depth. We assume three neutrino species, approximated as two massless states and a single massive neutrino of mass $m_\nu = 0.06 \text{ eV}$. We use uniform priors $\omega_b \in [0.018, 0.024]$, $\omega_c \in [0.10, 0.14]$, $100 \theta_s \in [1.03, 1.05]$, $\ln(10^{10} A_s) \in [3.0, 3.18]$, $n_s \in [0.9, 1.1]$, and $\tau_{\text{reio}} \in [0.04, 0.125]$ for the common free parameters, and $z_{\dagger} \in [1, 3]$ for the additional free parameter of Λ_s CDM. Also, we use uniform priors $S_8 \in [0.1, 1.3]$ and $h \in [0.64, 0.82]$ for relevant analyses. In Table I, we show observational constraints on the parameters of both the Λ_s CDM and Λ CDM models from different data combinations. Fig. 1 displays two-dimensional marginalized probability posteriors of z_{\dagger} versus H_0 , M_B , S_8 , $D_H(2.33)/r_d$ (D_H/r_d at $z_{\text{eff}} = 2.33$ relevant to the Ly- α measurements), t_0 , and ω_b in Λ_s CDM model for CMB+BAOtr+PP&SH0ES+KiDS-1000. Additionally, Table II quantifies the concordance/discordance between the Λ CDM/ Λ_s CDM models and the theoretical/direct observational estimations, viz., $H_0 = 73.04 \pm 1.04 \text{ km s}^{-1} \text{ Mpc}^{-1}$ (SH0ES) [1]; $M_B = -19.244 \pm 0.037 \text{ mag}$ (SH0ES) [2]; $D_H(2.33)/r_d = 8.99 \pm 0.19$ (for the combined Ly- α data) [3]; $t_0 = 13.50 \pm 0.15 \text{ Gyr}$ (systematic uncertainties are not included) [4]; $10^2 \omega_b^{\text{LUNA}} = 2.233 \pm 0.036$ (empirical approach, based primarily on experimentally measured cross sections for $d(p, \gamma)^3\text{He}$ reaction) [5] and $10^2 \omega_b^{\text{PCUV21}} = 2.195 \pm 0.022$ (theoretical approach, incorporating nuclear theory for $d(p, \gamma)^3\text{He}$ reaction) [6]. $S_8 = 0.746_{-0.021}^{+0.026}$ (Λ_s CDM: KiDS-1000) and $S_8 = 0.749_{-0.020}^{+0.027}$ (Λ CDM: KiDS-1000) obtained in this work.

TRIANGLE POSTERIORS

In Fig. 2-8, we present the One- and two-dimensional (at 68% and 95% CL) marginalized distributions of the model parameters for both models. We do not see strong correlations between z_{\dagger} and the six baseline parameters, but these exist among z_{\dagger} , H_0 , M_B , S_8 , and Ω_m . Thus, triangular plots showing the joint posteriors between the parameters present extra complementary information to the tables in the main text.

* akarsuo@itu.edu.tr

† e.divalentino@sheffield.ac.uk

‡ suresh.math@igu.ac.in

§ rafadcnunes@gmail.com

¶ javazquez@icf.unam.mx

** anita.math.rs@igu.ac.in

- [1] A. G. Riess *et al.*, A Comprehensive Measurement of the Local Value of the Hubble Constant with $1 \text{ km s}^{-1} \text{ Mpc}^{-1}$ Uncertainty from the Hubble Space Telescope and the SH0ES Team, *Astrophys. J. Lett.* **934**, L7 (2022), arXiv:2112.04510 [astro-ph.CO].
- [2] D. Camarena and V. Marra, On the use of the local prior on the absolute magnitude of Type Ia supernovae in cosmological inference, *Mon. Not. Roy. Astron. Soc.* **504**, 5164 (2021), arXiv:2101.08641 [astro-ph.CO].
- [3] H. du Mas des Bourboux *et al.*, The Completed SDSS-IV Extended Baryon Oscillation Spectroscopic Survey: Baryon Acoustic Oscillations with Ly α Forests, *Astrophys. J.* **901**, 153 (2020), arXiv:2007.08995 [astro-ph.CO].
- [4] D. Valcin, R. Jimenez, L. Verde, J. L. Bernal, and B. D. Wandelt, The age of the Universe with globular clusters: reducing systematic uncertainties, *JCAP* **08**, 017, arXiv:2102.04486 [astro-ph.GA].
- [5] V. Mossa *et al.*, The baryon density of the Universe from an improved rate of deuterium burning, *Nature* **587**, 210 (2020).
- [6] C. Pitrou, A. Coc, J.-P. Uzan, and E. Vangioni, A new tension in the cosmological model from primordial deuterium?, *Mon. Not. Roy. Astron. Soc.* **502**, 2474 (2021), arXiv:2011.11320 [astro-ph.CO].

TABLE I. Marginalized constraints, mean values with 68% CL (bestfit value), on the free and some derived parameters of the Λ_s CDM and standard Λ CDM models for different data set combinations. Bayes factors \mathcal{B}_{ij} given by $\ln \mathcal{B}_{ij} = \ln \mathcal{Z}_{\Lambda\text{CDM}} - \ln \mathcal{Z}_{\Lambda_s\text{CDM}}$ are also displayed for the different analyses, so that a negative value indicates a preference for the Λ_s CDM model against the Λ CDM scenario.

Data set	Planck	Planck+BAOtr	Planck+BAOtr +PP	Planck+BAOtr +PP&SHOES	Planck+BAOtr +PP&SHOES+KiDS-1000
Model	Λ_s CDM ACDM	Λ_s CDM ACDM	Λ_s CDM ACDM	Λ_s CDM ACDM	Λ_s CDM ACDM
$10^2\omega_b$	$2.241 \pm 0.015(2.252)$ $2.238 \pm 0.014(2.235)$	$2.249 \pm 0.014(2.251)$ $2.262 \pm 0.014(2.255)$	$2.245 \pm 0.014(2.247)$ $2.256 \pm 0.013(2.248)$	$2.246 \pm 0.014(2.249)$ $2.277 \pm 0.013(2.280)$	$2.250 \pm 0.013(2.252)$ $2.282 \pm 0.013(2.283)$
ω_{cdm}	$0.1195 \pm 0.0012(0.1187)$ $0.1200 \pm 0.0012(0.1202)$	$0.1187 \pm 0.0012(0.1186)$ $0.1169 \pm 0.0010(0.1173)$	$0.1192 \pm 0.0011(0.1198)$ $0.1175 \pm 0.0010(0.1174)$	$0.1192^{+0.0010}_{-0.0012}(0.1186)$ $0.1154 \pm 0.0009(0.1151)$	$0.1184 \pm 0.0010(0.1180)$ $0.1149 \pm 0.0008(0.1143)$
$100\theta_s$	$1.04189 \pm 0.00029(1.04207)$ $1.04190^{+0.00027}_{-0.00031}(1.04178)$	$1.04199 \pm 0.00030(1.04194)$ $1.04218 \pm 0.00028(1.04211)$	$1.04196 \pm 0.00029(1.04181)$ $1.04213 \pm 0.00027(1.04225)$	$1.04197 \pm 0.00029(1.04167)$ $1.04236 \pm 0.00028(1.04242)$	$1.04199 \pm 0.00031(1.04168)$ $1.04242 \pm 0.00029(1.04218)$
$\ln(10^{10}A_s)$	$3.040 \pm 0.014(3.046)$ $3.046 \pm 0.014(3.049)$	$3.039 \pm 0.015(3.034)$ $3.058^{+0.014}_{-0.017}(3.053)$	$3.042 \pm 0.014(3.044)$ $3.056 \pm 0.016(3.047)$	$3.039 \pm 0.014(3.038)$ $3.064^{+0.015}_{-0.017}(3.063)$	$3.037 \pm 0.014(3.045)$ $3.062^{+0.013}_{-0.016}(3.079)$
n_s	$0.9669 \pm 0.0043(0.9664)$ $0.9657 \pm 0.0041(0.9658)$	$0.9695 \pm 0.0041(0.9692)$ $0.9733 \pm 0.0039(0.9706)$	$0.9679 \pm 0.0039(0.9644)$ $0.9715 \pm 0.0035(0.9728)$	$0.9682 \pm 0.0040(0.9711)$ $0.9768 \pm 0.0038(0.9801)$	$0.9695 \pm 0.0043(0.9701)$ $0.9786 \pm 0.0035(0.9797)$
τ_{reio}	$0.0528 \pm 0.0073(0.0569)$ $0.0550 \pm 0.0072(0.5488)$	$0.0532 \pm 0.0077(0.0515)$ $0.0639^{+0.0073}_{-0.0087}(0.0608)$	$0.0534 \pm 0.0073(0.0544)$ $0.0624^{+0.0074}_{-0.0086}(0.0586)$	$0.0522 \pm 0.0073(0.0555)$ $0.0684^{+0.0076}_{-0.0089}(0.0685)$	$0.0525 \pm 0.0074(0.0584)$ $0.0678^{+0.0067}_{-0.0085}(0.0771)$
z_{\dagger}	unconstrained	$1.70^{+0.09}_{-0.19}(1.65)$	$1.87^{+0.13}_{-0.21}(1.75)$	$1.70^{+0.10}_{-0.13}(1.67)$	$1.72^{+0.09}_{-0.12}(1.70)$
z_{reio}	$7.43^{+0.78}_{-0.67}(7.83)$ $7.75 \pm 0.72(7.76)$	$7.42 \pm 0.78(7.25)$ $8.52 \pm 0.76(8.25)$	$7.47 \pm 0.74(7.59)$ $8.39 \pm 0.76(8.05)$	$7.34 \pm 0.76(7.67)$ $8.87 \pm 0.75(8.88)$	$7.34 \pm 0.74(7.94)$ $8.79^{+0.64}_{-0.75}(9.64)$
Y_P	$0.247856 \pm 0.000063(0.247905)$ $0.247842 \pm 0.000062(0.247832)$	$0.247889 \pm 0.000060(0.247901)$ $0.247944 \pm 0.000059(0.247914)$	$0.247876 \pm 0.000058(0.247881)$ $0.247921^{+0.000059}_{-0.000053}(0.247888)$	$0.247877 \pm 0.000061(0.247887)$ $0.248010 \pm 0.000056(0.248020)$	$0.247895 \pm 0.000057(0.247903)$ $0.248031 \pm 0.000055(0.248034)$
z_d	$1060.03 \pm 0.29(1060.22)$ $1059.99 \pm 0.28(1059.95)$	$1060.15 \pm 0.29(1060.22)$ $1060.28 \pm 0.28(1060.16)$	$1060.12 \pm 0.29(1060.19)$ $1060.21 \pm 0.27(1060.03)$	$1060.12 \pm 0.30(1060.15)$ $1060.52 \pm 0.28(1060.55)$	$1060.15 \pm 0.27(1060.16)$ $1060.59 \pm 0.29(1060.56)$
r_d [Mpc]	$147.17 \pm 0.27(147.28)$ $147.07^{+0.24}_{-0.25}(147.06)$	$147.31 \pm 0.26(147.30)$ $147.65 \pm 0.25(147.63)$	$147.20 \pm 0.25(147.03)$ $147.55^{+0.24}_{-0.21}(147.65)$	$147.21 \pm 0.24(147.33)$ $147.87 \pm 0.23(147.93)$	$147.36 \pm 0.23(147.46)$ $147.96^{+0.25}_{-0.23}(148.10)$
t_0 [Gyr]	$13.620^{+0.120}_{-0.042}(13.596)$ $13.793 \pm 0.023(13.800)$	$13.517^{+0.038}_{-0.049}(13.502)$ $13.745 \pm 0.021(13.756)$	$13.576^{+0.039}_{-0.034}(13.560)$ $13.755 \pm 0.020(13.760)$	$13.531 \pm 0.028(13.524)$ $13.716 \pm 0.020(13.710)$	$13.522 \pm 0.027(13.521)$ $13.706 \pm 0.018(13.709)$
M_B [mag]	--	--	$-19.317^{+0.021}_{-0.025}(-19.311)$ $-19.407 \pm 0.013(-19.411)$	$-19.290 \pm 0.017(-19.278)$ $-19.379 \pm 0.012(-19.373)$	$-19.282 \pm 0.017(-19.280)$ $-19.372 \pm 0.011(-19.369)$
H_0 [km/s/Mpc]	$70.77^{+0.79}_{-2.70}(71.22)$ $67.39 \pm 0.55(67.28)$	$73.30^{+1.20}_{-1.00}(73.59)$ $68.84 \pm 0.48(68.61)$	$71.72^{+0.73}_{-0.92}(71.97)$ $68.55 \pm 0.44(68.54)$	$72.82 \pm 0.65(73.20)$ $69.57 \pm 0.42(69.73)$	$73.16 \pm 0.64(73.36)$ $69.83 \pm 0.37(69.96)$
ω_m	$0.1426 \pm 0.0011(0.1418)$ $0.1431 \pm 0.0011(0.1432)$	$0.1418 \pm 0.0011(0.1418)$ $0.1401 \pm 0.0010(0.1405)$	$0.1423 \pm 0.0010(0.1429)$ $0.1407 \pm 0.0010(0.1406)$	$0.1422 \pm 0.0010(0.1418)$ $0.1388 \pm 0.0009(0.1385)$	$0.1416 \pm 0.0010(0.1411)$ $0.1384 \pm 0.0008(0.1378)$
Ω_m	$0.2860^{+0.0230}_{-0.0099}(0.2796)$ $0.3151 \pm 0.0075(0.3163)$	$0.2643^{+0.0072}_{-0.0090}(0.2618)$ $0.2958 \pm 0.0061(0.2984)$	$0.2768^{+0.0072}_{-0.0063}(0.2759)$ $0.2995 \pm 0.0056(0.2992)$	$0.2683 \pm 0.0052(0.2646)$ $0.2869 \pm 0.0051(0.2849)$	$0.2646 \pm 0.0052(0.2622)$ $0.2837 \pm 0.0045(0.2816)$
σ_8	$0.8210^{+0.0064}_{-0.0110}(0.8191)$ $0.8121^{+0.0055}_{-0.0061}(0.8136)$	$0.8278 \pm 0.0086(0.8260)$ $0.8076^{+0.0058}_{-0.0067}(0.8064)$	$0.8240 \pm 0.0074(0.8281)$ $0.8087 \pm 0.0062(0.8054)$	$0.8277 \pm 0.0075(0.8274)$ $0.8054 \pm 0.0064(0.8047)$	$0.8244 \pm 0.0067(0.8264)$ $0.8030 \pm 0.0055(0.8076)$
S_8	$0.801^{+0.026}_{-0.016}(0.791)$ $0.832 \pm 0.013(0.835)$	$0.777 \pm 0.011(0.772)$ $0.802 \pm 0.011(0.804)$	$0.791 \pm 0.011(0.794)$ $0.808 \pm 0.010(0.804)$	$0.783 \pm 0.010(0.777)$ $0.788 \pm 0.010(0.784)$	$0.774 \pm 0.009(0.773)(0.773)$ $0.781 \pm 0.008(0.782)$
$D_H(2.33)/r_d$	$8.960^{+0.280}_{-0.380}(9.218)$ $8.615 \pm 0.013(8.614)$	$9.240^{+0.035}_{-0.025}(9.252)$ $8.648 \pm 0.011(8.643)$	$9.201^{+0.041}_{-0.017}(9.222)$ $8.641 \pm 0.010(8.639)$	$9.232 \pm 0.025(9.242)$ $8.664 \pm 0.008(8.667)$	$9.249 \pm 0.025(9.261)$ $8.670 \pm 0.008(8.675)$
χ^2_{\min}	2778.06 2780.52	2793.38 2820.30	4219.68 4235.18	4097.32 4138.26	4185.34 4226.50
$\ln \mathcal{Z}$	-1423.17 -1424.45	-1432.71 -1445.36	-2144.75 -2152.27	-2084.37 -2103.84	-2133.85 -2153.62
$\ln \mathcal{B}_{ij}$	-1.28	-12.65	-7.52	-19.47	-19.77

TABLE II. Concordance/discordance between the Λ CDM/ Λ_s CDM models and the theoretical/direct observational estimations, viz., $H_0 = 73.04 \pm 1.04 \text{ km s}^{-1} \text{ Mpc}^{-1}$ (SH0ES) [1]; $M_B = -19.244 \pm 0.037 \text{ mag}$ (SH0ES) [2]; $D_H(2.33)/r_d = 8.99 \pm 0.19$ (for the combined Ly- α data) [3]; $t_0 = 13.50 \pm 0.15 \text{ Gyr}$ (systematic uncertainties are not included) [4]; $10^2 \omega_b^{\text{LUNA}} = 2.233 \pm 0.036$ (empirical approach, based primarily on experimentally measured cross sections for $d(p, \gamma)^3\text{He}$ reaction) [5] and $10^2 \omega_b^{\text{PCUV21}} = 2.195 \pm 0.022$ (theoretical approach, incorporating nuclear theory for $d(p, \gamma)^3\text{He}$ reaction) [6]. $S_8 = 0.746^{+0.026}_{-0.021}$ (Λ_s CDM: KiDS-1000) and $S_8 = 0.749^{+0.027}_{-0.020}$ (Λ CDM: KiDS-1000) obtained in this work.

Data set	Planck	Planck+BAOtr	Planck+BAOtr	Planck+BAOtr	Planck+BAOtr
	Λ_s CDM	Λ_s CDM	Λ_s CDM	Λ_s CDM	Λ_s CDM
Model	Λ CDM	Λ CDM	Λ CDM	Λ CDM	Λ CDM
H_0	1.4σ	0.2σ	1.0σ	0.2σ	0.1σ
	4.8σ	3.7σ	4.3σ	3.1σ	2.9σ
M_B	–	–	1.7σ	1.1σ	0.9σ
	–	–	4.5σ	3.5σ	3.3σ
S_8	1.7σ	1.2σ	1.7σ	1.4σ	1.1σ
	3.1σ	2.0σ	2.3σ	1.5σ	1.3σ
t_0	1.0σ	0.1σ	0.5σ	0.2σ	0.1σ
	1.9σ	1.6σ	1.7σ	1.4σ	1.4σ
$D_H(2.33)/r_d$	0.2σ	1.3σ	1.1σ	1.3σ	1.4σ
	2.0σ	1.8σ	1.8σ	1.7σ	1.7σ
ω_b^{PCUV21}	1.2σ	2.1σ	1.9σ	1.9σ	2.2σ
	1.6σ	2.6σ	2.4σ	3.1σ	3.4σ
ω_b^{LUNA}	0.3σ	0.4σ	0.3σ	0.3σ	0.4σ
	0.1σ	0.8σ	0.6σ	1.1σ	1.3σ

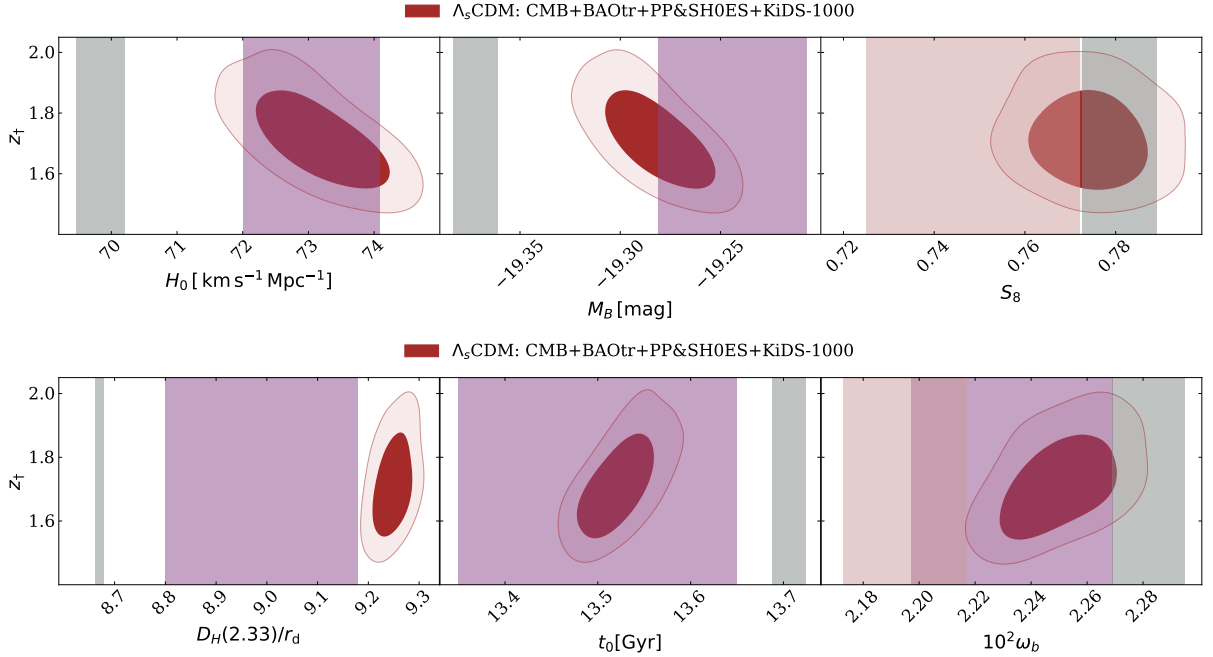


FIG. 1. Two-dimensional marginalized probability posteriors of z_{\dagger} versus H_0 , M_B , S_8 , $D_H(2.33)/r_d$ (D_H/r_d at $z_{\text{eff}} = 2.33$ relevant to the Ly- α measurements), t_0 , and ω_b in Λ_s CDM model for CMB+BAOtr+PP&SH0ES+KiDS-1000. The vertical grey bands are the constraints (68% CL) for the Λ CDM model. The vertical purple bands stand for the theoretical/direct observational estimations (at 68% CL) of the corresponding parameters commonly used in the literature: $H_0 = 73.04 \pm 1.04 \text{ km s}^{-1} \text{ Mpc}^{-1}$ (SH0ES) [1]; $M_B = -19.244 \pm 0.037 \text{ mag}$ (SH0ES) [2]; $D_H(2.33)/r_d = 8.99 \pm 0.19$ (for combined Ly- α data) [3]; $t_0 = 13.50 \pm 0.15 \text{ Gyr}$ (systematic uncertainties are not included) [4]; $10^2 \omega_b^{\text{LUNA}} = 2.233 \pm 0.036$ [5]. In addition, we show vertical brown band for $10^2 \omega_b^{\text{PCUV21}} = 2.195 \pm 0.022$ [6] and $S_8 = 0.746^{+0.026}_{-0.021}$ (Λ_s CDM: KiDS-1000) [this work].

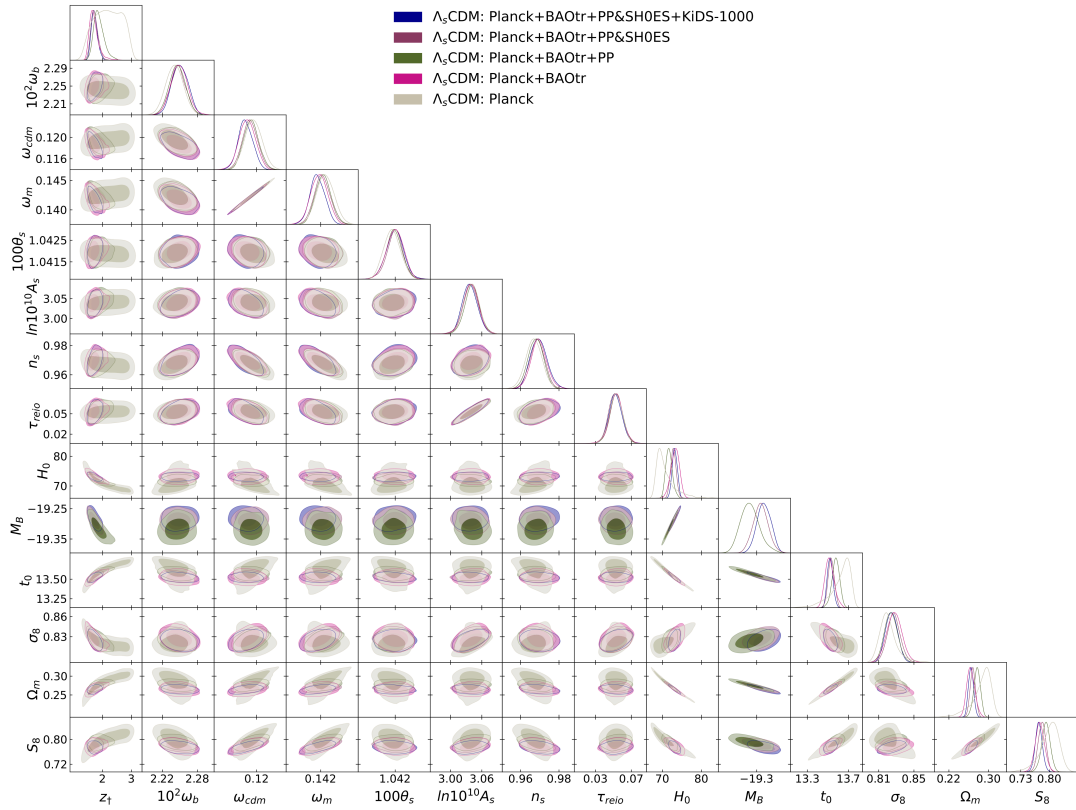


FIG. 2. One- and two-dimensional (68% and 95% CLs) marginalized distributions of the Λ_s CDM model parameters from Planck, Planck+BAOtr, Planck+BAOtr+PP, Planck+BAOtr+PP&SH0ES, and Planck+BAOtr+PP&SH0ES+KiDS-1000.

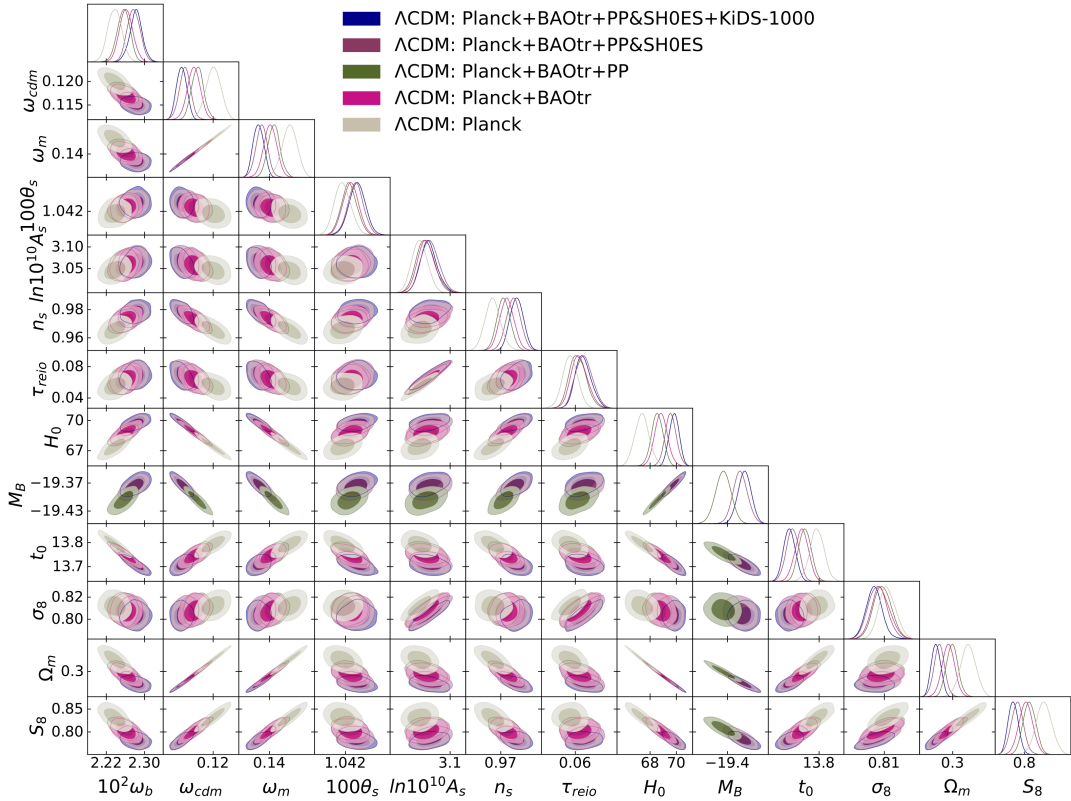


FIG. 3. One- and two-dimensional (68% and 95% CLs) marginalized distributions of the Λ CDM model parameters from Planck, Planck+BAOtr, Planck+BAOtr+PP, Planck+BAOtr+PP&SH0ES, and Planck+BAOtr+PP&SH0ES+KiDS-1000.

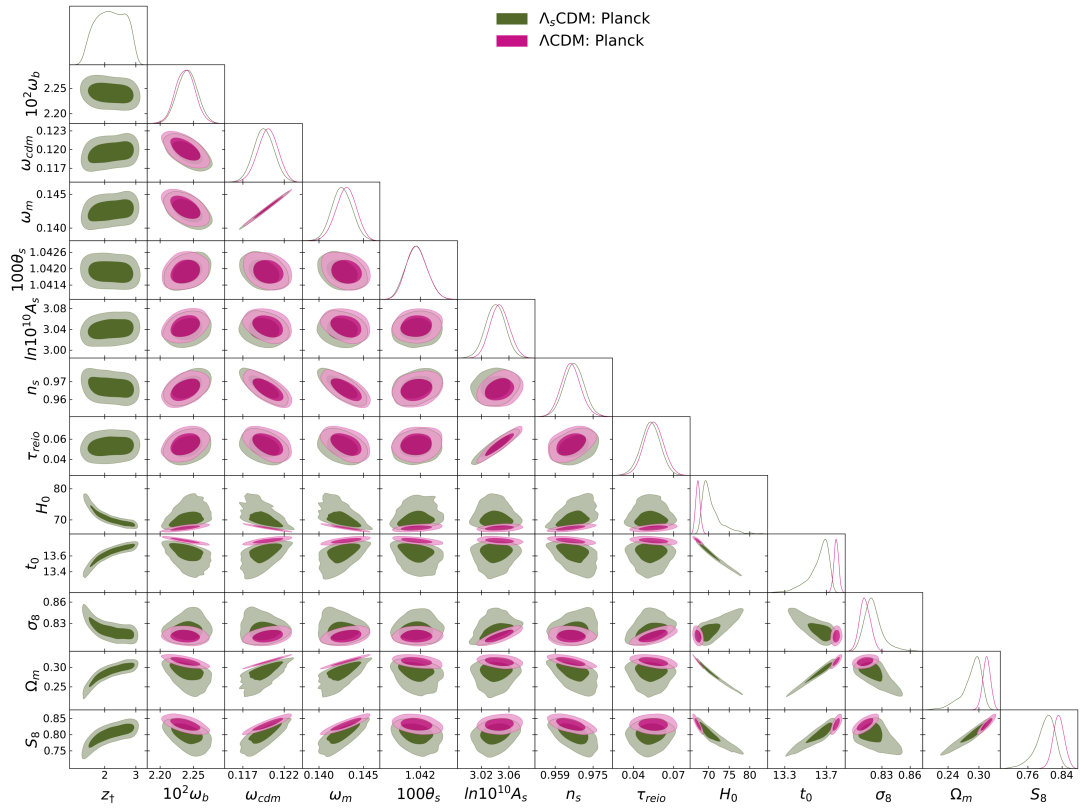


FIG. 4. One- and two-dimensional (68% and 95% CLs) marginalized distributions of the model parameters from Planck.

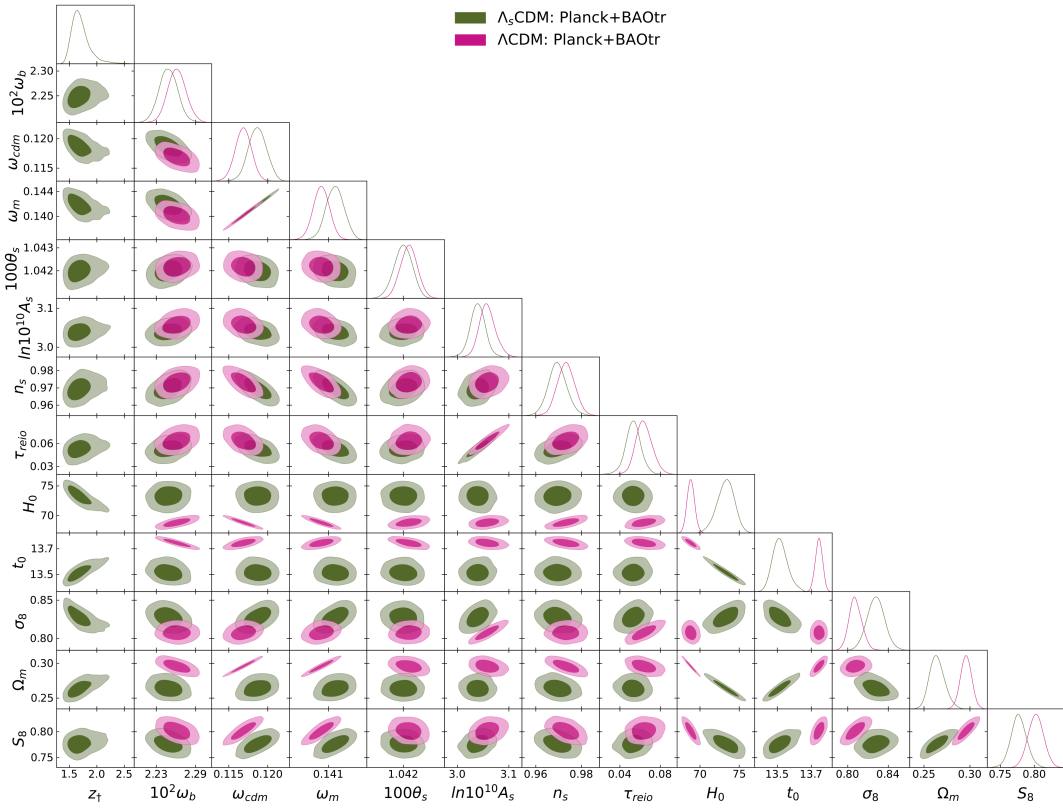


FIG. 5. One- and two-dimensional (68% and 95% CLs) marginalized distributions of the model parameters from Planck+BAOtr.

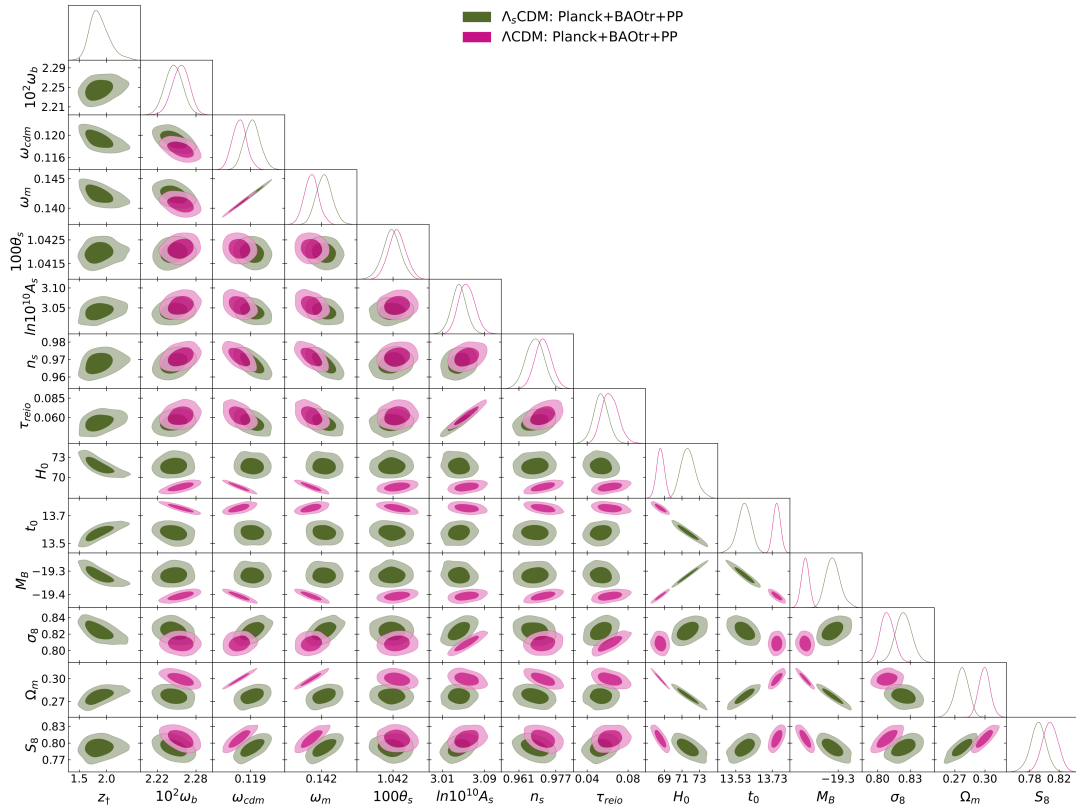


FIG. 6. One- and two-dimensional (68% and 95% CLs) marginalized distributions of the model parameters from Planck+BAOtr+PP.

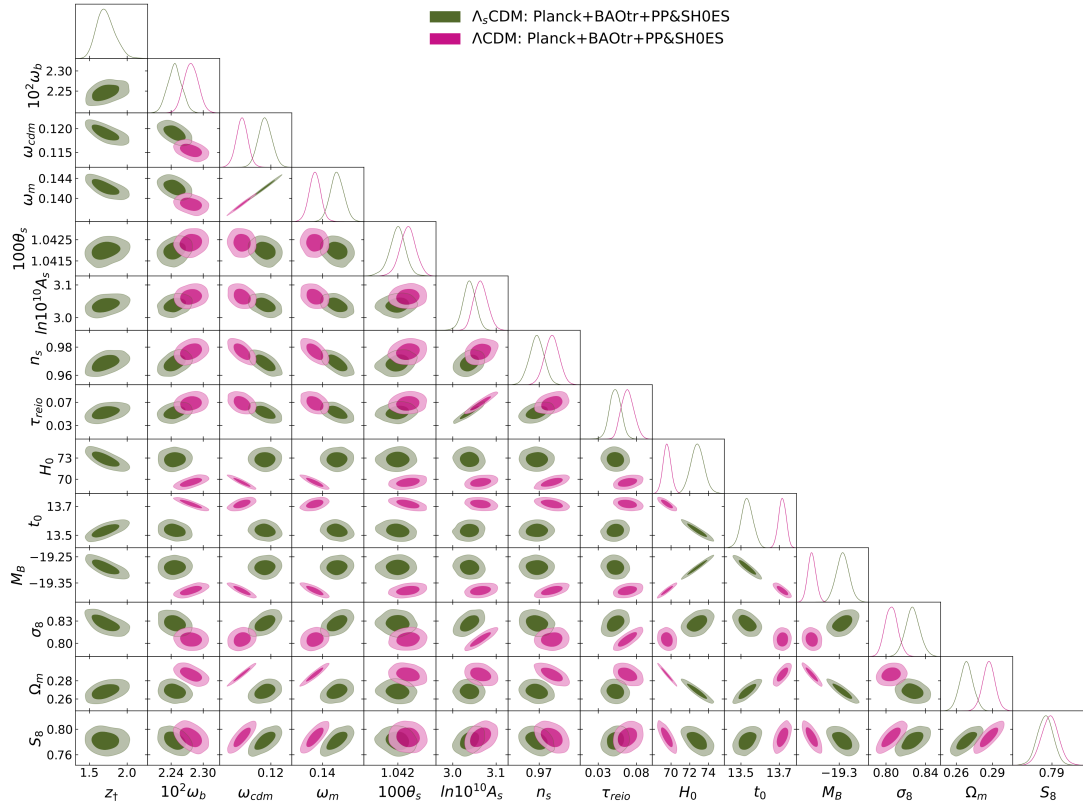


FIG. 7. One- and two-dimensional (68% and 95% CLs) marginalized distributions of the model parameters from Planck+BAOtr+PP&SH0ES.

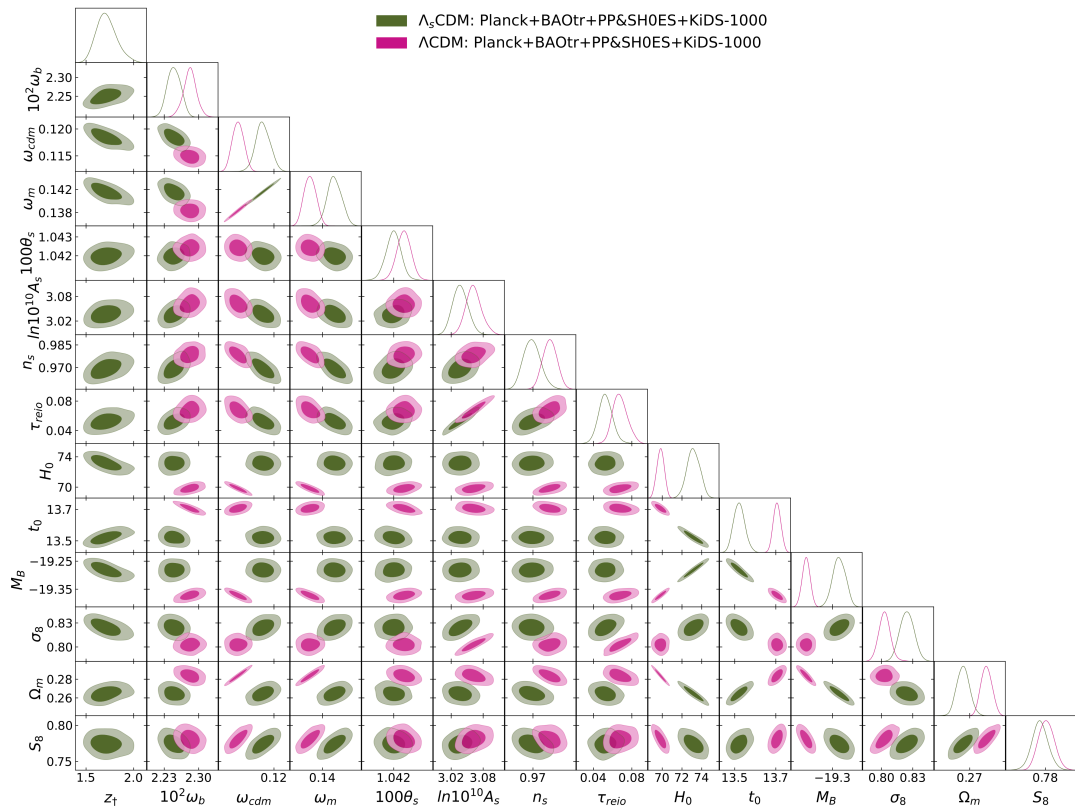


FIG. 8. One- and two-dimensional (68% and 95% CLs) marginalized distributions of the model parameters from Planck+BAOtr+PP &SH0ES+KiDS-1000.